Oxygen Binding and Activation: Early Steps in the Reaction of Oxygen with Cytochrome *c* Oxidase†

Michael I. Verkhovsky,*,‡ Joel E. Morgan, and Mårten Wikström

Helsinki Bioenergetics Group, Department of Medical Chemistry, P.O. Box 8 (Siltavuorenpenger 10A), University of Helsinki, FI-00014 Helsinki, Finland

Received August 30, 1993; Revised Manuscript Received December 29, 1993®

ABSTRACT: We have studied the flow–flash reaction of fully reduced cytochrome *c* oxidase with a high concentration of oxygen (1 mM), recording the first 200 μs of the reaction at a number of wavelengths between 400 and 455 nm. This approach has allowed us to observe kinetic phases with time constants of 8 and 32 μs and to separate their spectra. The spectrum of the first phase is comparable to that of oxygen binding to myoglobin, while the spectrum of the second phase appears to contain a contribution from a peroxy intermediate. The results are discussed in the context of a model in which the 8-μs phase reflects the establishment of an equilibrium of oxygen-bound states, while the 32-μs phase arises when this system is trapped as a peroxy intermediate, by inter-heme electron transfer.

Aerobic organisms are, by definition, those that obtain energy for their life processes by consuming oxygen. In order to do this, an organism must solve three major problems: First, oxygen is quite inert, and even though a great deal of energy is released when oxygen is reduced to water, this process does not proceed at an appreciable rate without activation or catalysis. Second, virtually all of the intermediates on the pathway from oxygen to water (superoxide, peroxide, and hydroxyl radicals) are hazardous to the cell; respiration must avoid producing them or ensure that they are not released. Third, in order for this process to be useful to the cell, the energy released by this redox reaction must be conserved in a form that can be used by the energy-requiring cellular processes.

In eukaryotic organisms, this reaction is the responsibility of cytochrome *c* oxidase,[1] the terminal enzyme in the mitochondrial respiratory chain [for a basic review, see Wikström et al. (1981)]. In this enzyme, oxygen is reduced to water using electrons derived from metabolism. Energy is conserved as an electrochemical proton gradient across the mitochondrial inner membrane, which is ultimately used to generate ATP. Cytochrome *c* oxidase is a very effective catalyst. The enzyme is capable of reducing well over 100 oxygen molecules to water every second, and some of the individual steps in the reaction are far faster. The actual catalysis of the oxygen reaction takes place at a binuclear site made up of a heme and a copper ion (Fe_{a3} and Cu_B).[2] Another heme and another copper (Fe_a and Cu_A) serve as electron carriers en route from cytochrome *c*, the immediate electron donor, to this site.

One way to approach the question of how cytochrome *c* oxidase accomplishes its task is to try to observe individual steps in the enzyme's reaction and describe them in chemical terms. The oxidative part of enzyme turnover can be modeled by reacting the fully (four-electron) reduced enzyme with oxygen. However, this reaction is too fast to be resolved by rapid mixing techniques. In order overcome this problem, Gibson and Greenwood (1963) devised the, now classical, "flow–flash" technique. A conventional stopped-flow instrument is used to mix cytochrome *c* oxidase with oxygen, but the enzyme is blocked by carbon monoxide at the catalytic site, and the reaction with oxygen can begin only when the CO is removed by a flash of light. This improves time resolution in the experiment from milliseconds to nanoseconds.

The picture of the reaction which has emerged from flow–flash and other studies is the subject of a recent review by Babcock and Wikström (1992) and may be briefly described as follows: By analogy to carbon monoxide, oxygen is thought to enter the enzyme by binding to Cu_B. Within the first 20 μs of the reaction, a ferrous–oxy intermediate (**A**) is observed optically and in resonance Raman measurements. The initial oxidation of both hemes follows with a time constant of about 30 μs (Hill, 1991), and a ferric–peroxy intermediate (**P**) is observed by resonance Raman spectroscopy in the time range of 160–220 μs. The initial oxidation of Cu_A is observed with a time constant of about 170 μs, and a ferryl intermediate (**F**) is detected by resonance Raman at about 500 μs. Finally, the remaining populations of reduced heme and Cu_A oxidize with a rate of about 1000 s^{-1}, resulting in a fully oxidized state (**O**). This sequence of intermediates is only an outline of the reaction mechanism, and significant questions remain as to the protonation steps, the factors that control the rates of various steps, and the correlation between the electron-transfer events and the oxygen intermediates.

This article presents a new set of flow–flash experiments focusing on the early events in the oxygen reaction. We have studied the reaction of the fully reduced enzyme with a high concentration of oxygen, recording the first 200 μs of the reaction at a number of wavelengths between 400 and 455 nm. This approach has allowed us to observe and separate

† This work has been supported by research grants from the Sigrid Jusèlius Foundation, the Academy of Finland, and the University of Helsinki.

* Author to whom correspondence should be addressed at the University of Helsinki. E.mail: mverkhovsky@cc.helsinki.fi. Fax: (358-0) 191-8276.

‡ On leave from the A. N. Belozersky Institute of Physico-Chemical Biology, Moscow State University, Moscow, 119899, Russia.

® Abstract published in *Advance ACS Abstracts,* February 15, 1994.

[1] EC 1.9.3.1.

[2] Abbreviations: **A**, ferrous–oxy intermediate; **B**, Cu_B–oxy intermediate; **F**, ferryl intermediate; Fe_a, the low-spin heme; Fe_{a3}, the oxygen-binding heme; k_{app}, apparent rate constant; $K_{D,app}$, apparent dissociation constant; **O**, fully oxidized enzyme; **P**, ferric–peroxy intermediate (in general); **P1**, unprotonated ferric–peroxy intermediate shown in Figure 4; **P/S**, peroxy or superoxy intermediate; **R**, unliganded, fully reduced enzyme; τ, kinetic time constant.

0006-2960/94/0433-3079$04.50/0

kinetic phases with rate constants of 1.22×10^5 and 0.32×10^5 s^{-1} and to deduce their spectra. The results clearly show the formation of a ferrous–oxy intermediate as a product of the first kinetic phase and provide evidence of a peroxy compound as the immediate product of the second reaction phase. They also shed light on the possibility that oxygen binds to Cu_B en route to the oxygen-binding heme. To explain these and other recent results, a new model for the early steps in the reaction of O_2 with cytochrome *c* oxidase is proposed.

MATERIALS AND METHODS

Reagents and Enzymes. Bovine heart cytochrome *c* oxidase was prepared by a modification of the method of Hartzell and Beinert (1974). During enzyme preparation, the pH was kept above 7.8 (Baker et al., 1987). No ethanol was used to remove the Triton X-114 following the red/green cut; instead, the green pellet was repeatedly resuspended in the preparation buffer (without ethanol) and centrifuged, until the amount of detergent was too small to cause the supernatant to bubble when shaken. Equine cytochrome *c* (type III) and sperm whale myoglobin (type II) were from Sigma.

Flow–Flash Apparatus. The mixing system was a manually operated stopped-flow system designed to be used with a third party spectrophotometer (Hi-tech, Salisbury, England, Model SFA-11) modified as follows: gas-tight syringes (Hamilton) were used as driving syringes (1 mL for enzyme solution and 5 mL for oxygenated buffer); the valve to which the enzyme syringe was attached was replaced with a gas-tight, three-way valve (Hamilton); the umbilical connection to the cuvette was removed, and the cuvette (which has a built-in mixer) was attached directly to the syringe valves, using the original tubing, but reducing the length to a minimum (about 10 cm). The timing system was triggered by the stop syringe, using a 100-ms delay for mixing. The details of the transient absorbance measurement system have been published previously (Morgan et al., 1993).

Sample Preparation and Handling. The flow system was made anaerobic by washing with a strong solution of sodium dithionite. When necessary, the dithionite was removed by rinsing with anaerobic water. Enzyme samples and anaerobic water were prepared on the vacuum line using a 50-mL spherical flask with a small side arm. Cytochrome *c* oxidase, in buffer, at the appropriate concentration was placed in the flask, together with a glass-covered magnetic stir bar. A solution containing cytochrome *c* and ascorbate was placed in the side arm. The contents of the flask were made anaerobic by repeated washings with anaerobic argon. The argon was then replaced by an atmosphere of CO, and the contents of the side arm were mixed into the main flask. Enzyme samples were transferred from the vacuum line flask to the driving syringe (1-mL Hamilton) through a long needle connected to the third port of the syringe control valve. An argon counterflow was used to maintain anaerobicity.

Data Acquisition. Two sets of kinetic data were acquired at each wavelength: reference data in which oxygen was *not* mixed into the sample, and measurement data in which oxygen was used. Since the reference sample does not require mixing, this provided stable reference values for the amplitude of the initial absorbance jump that could be used to normalize the amplitudes in the measurement data.

To acquire the reference data, the small driving syringe was filled with an enzyme sample, and the large syringe was filled with a solution of dithionite in buffer. The cuvette was placed in a conventional scanning spectrophotometer, and the mixer was operated to flush out the flow system between the syringes and the cuvette with enzyme and buffer and to ensure uniform mixing. This was repeated until operation of the mixer did not change the spectrum. The cuvette was then moved to the transient absorbance instrument, and all of the reference data (all wavelengths) were recorded without further sample mixing. Typically, 20–30 transients were averaged for each wavelength.

To acquire the measurement data, the large syringe was rinsed to remove the dithionite solution and then filled with oxygen-saturated buffer. The small syringe was then refilled with enzyme sample, and the cuvette was placed in the transient absorbance instrument. The mixer was then operated several times to flush out the flow system (as above). Each time the mixer was operated, a flow–flash transient was measured. Once a consistent signal was obtained (usually after 2–4 shots), the remaining shots were recorded to memory. It was usually possible to acquire about 12 transients starting from full syringes. The syringes could then be refilled and acquisition started at a new wavelength.

Data Handling. In order to avoid possible errors due to mixing and oxygen leaks in the flow–flash experiments, the amplitudes of the measurement data were normalized with respect to the reference data, which were all acquired from a single anaerobic sample, by matching the absorbance jump at the point of photolysis. Analysis software: Graphic Interactive Management (Alexander Drachev, Tempe, AZ).

RESULTS AND DISCUSSION

The experiment begins when a flash from the laser breaks the Fe–CO bond, freeing the enzyme to react with oxygen. Figure 1A,B shows the resulting absorbance changes for several wavelengths. Photolysis of the Fe–CO bond is accompanied by a spin-state change and a large absorbance jump (the step at zero on the time axis). The absorbance changes that follow this arise from reaction of the enzyme with oxygen.

The traces clearly show two phases in this early part of the reaction. The 437.5-nm trace is dominated by the faster process ($\tau = 8$ μs), while the 432.5-nm trace is dominated by the slower process ($\tau = 32$ μs). At 435 nm the two processes have opposite directions. The importance of this spectral separation of phases is shown by the data at 445 nm, where both phases have the same direction. The data at this wavelength can be fit almost equally well with one- and two-exponential functions. It was only by knowing, from the data at other wavelengths, that two processes are present and knowing their time constants that we were able to use a two-exponential fit to extract the amplitudes of the two phases at this wavelength. In a similar way, we determined the amplitudes of the two phases at a number of wavelengths and calculated their spectra (Figure 2).

First Kinetic Phase. Consistent with previous assignments (Oliveberg et al., 1989; see below), the fast phase appears to be the binding of oxygen to reduced Fe_{a3}. The top panel (A) of Figure 3 shows the spectrum of the fast kinetic phase (solid line) copied from Figure 2, together with a difference spectrum for the binding of CO to cytochrome *c* oxidase (an inverted spectrum of CO photolysis; dashed line). The fast phase spectrum has been multiplied by 1.6 in order to give the same amplitude at 445 nm as in the CO spectrum. For comparison, the lower panel (B) in Figure 3 shows difference spectra for the binding of oxygen (solid line) and CO (dashed line) to myoglobin, an enzyme with which both oxygen and CO form stable adducts. Although the cytochrome *c* oxidase spectra are both red-shifted compared to the myoglobin spectra, the relationship between the oxygen and CO spectra for the two

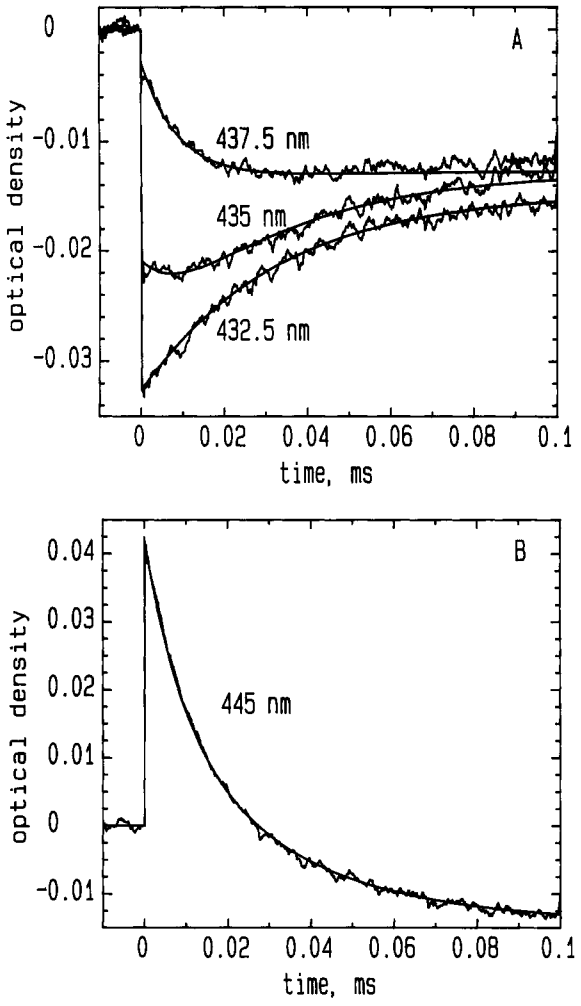

FIGURE 1: (A, B) Flow–flash reaction of fully reduced cytochrome *c* oxidase with oxygen–kinetic traces. Zero on the time scale is the point where the laser was fired. The noise-free curves are the results of fitting a two-exponential function (with time constants held at 8 and 32 μs) to the relaxation portion of the data (i.e., after the laser flash). Concentrations after mixing: cytochrome *c* oxidase, 2 μM; cytochrome *c*, 0.02 μM; ascorbate, 10 mM; oxygen, 1.0 mM; buffer, 40 mM Tris (pH 7.4), 400 mM NaCl, and 0.5% Tween-80. Temperature: 22 °C.

enzymes is qualitatively very similar. In the oxygen difference spectrum for cytochrome *c* oxidase, the maximum is less intense and closer by 2 nm to the maximum of the CO spectrum. Nevertheless, the basic similarity of the spectra confirms that a major product of the fast phase is indeed an Fe_{a3}–O_2 adduct.

The difference in amplitudes at 445 nm between the photolysis spectrum and the spectrum of the fast phase (the factor of 1.6 described above) indicates that not all of the unliganded, reduced Fe_{a3} produced by the laser flash binds oxygen in the fast phase of the reaction. Interestingly, this population of unbound Fe_{a3} finds a natural explanation in the model proposed below. However, the amount of this unbound Fe_{a3} may be overestimated. Comparison with the myoglobin spectra suggests that the absolute spectrum of the oxygen-bound species is broader than that of the CO-bound species, but in the case of cytochrome *c* oxidase, this oxygen spectrum is apparently less shifted and thus overlaps the 445 peak more. This would reduce the intensity of both negative and positive peaks in the difference spectrum in comparison with the CO-binding spectrum and, thus, account for part of the factor of 1.6 needed to equalize the 445-nm peak amplitudes in Figure 3A.

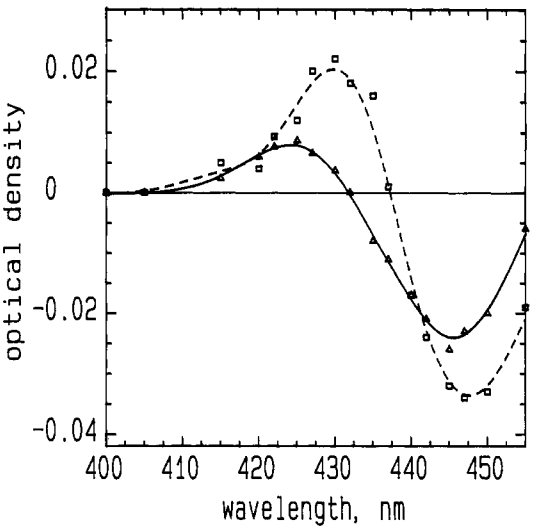

FIGURE 2: Spectra of the two phases: fast phase (τ = 8 μs), △ and —; slow phase (τ = 32 μs), □ and – –. The points show the amplitudes of the phases resulting from a two-exponential curve fit, while the curves are splines to the points. Conditions: see the legend to Figure 1.

Ferrous–Oxy Intermediate (A). The possibility of a ferrous–oxy intermediate was first proposed by Chance and co-workers (1975) on the basis of low-temperature kinetic studies. Early in the reaction, they observed a species which they assigned as a ferrous–oxy adduct, because its visible spectrum resembled that of oxygen binding to hemoglobin. They gave this intermediate the name "compound A". Later, an intermediate with a similar visible spectrum was identified in the early time difference spectra (20 μs – 5 μs) of the flow–flash reaction at room temperature (Orii, 1988a). Additional confirmation of this assignment came from resonance Raman studies of the flow–flash reaction, which revealed a signal at 20 μs with a Raman shift in the same range as those of other ferrous–oxy heme compounds (Varotsis et al., 1989).

However, attempts to observe the kinetics of formation of this ferrous–oxy intermediate were complicated by the low oxygen concentrations and time resolution available. In room-temperature experiments, the formation of this compound could be seen as a discrete process only when the starting material was the two-electron-reduced, mixed-valence enzyme (Hill & Greenwood, 1983). It was only when higher oxygen concentrations and better time resolution were introduced by the Göteborg group (Oliveberg et al., 1989) that the formation of the ferrous–oxy intermediate could be seen as an initial kinetic phase in the reaction of the fully reduced enzyme with oxygen, monitored at 445 nm.

The present data unify these observations. Using a multiple wavelength approach, we can resolve the binding of oxygen to Fe_{a3} as an unambiguous kinetic phase and, importantly, also estimate the population of the ferrous–oxy intermediate produced by this process (see below).

Second Kinetic Phase. The second kinetic phase has a time constant of 32 μs and a spectrum that is quite different from that of the fast phase (Figure 2). The spectrum has a minimum at 448 nm and a maximum at 430 nm. The position of the minimum is consistent with the oxidation of one or both of the hemes of the enzyme. The position of the maximum suggests the formation of either a ferric–peroxy or a ferryl intermediate. Both types of compounds might be expected to have maxima at about 430 nm (Vygodina & Konstantinov, 1988), but in all likelihood, this is a ferric–peroxy intermediate, since the ferryl compound (F) has been observed by resonance

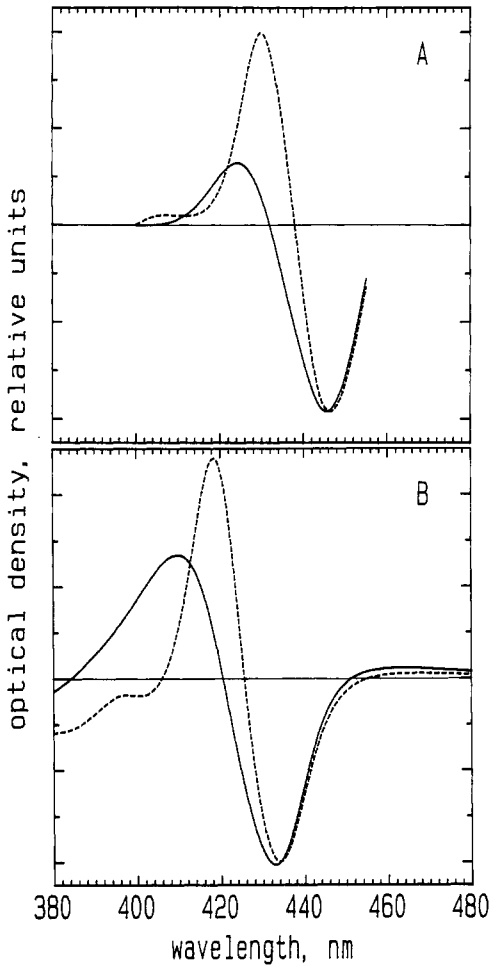

FIGURE 3: Spectra showing the similarity between the fast phase kinetic spectrum and the spectrum of oxygen binding to myoglobin. In both frames, the corresponding spectrum of CO binding is shown for reference. (A) —, kinetic spectrum of the fast phase (only the spline is shown; see Figure 2); - - -, spectrum of CO binding to reduced cytochrome *c* oxidase (an inverted spectrum of the initial photolysis absorbance jump from the same kinetic traces). The amplitude of the flow–flash kinetic spectrum has been multiplied by 1.6 (see text). (B) —, difference spectrum of oxygen binding to myoglobin; - - -, difference spectrum of CO binding to myoglobin. Buffer for myoglobin experiment: 50 mM HEPES (pH 7.5)/5 mM ascorbate.

Raman studies (Varotsis et al., 1993) only at a point much later in the reaction (500 μs). Most other possible assignments can be discounted. If unliganded, high-spin ferric Fe_{a3} were formed, it would produce a maximum near 415 nm. The low-spin heme does, in fact, become at least partly oxidized during this phase (Hill & Greenwood, 1984), but this gives rise to an absorbance increase at 425 nm and not at 430 nm.

Ferric–Peroxy Intermediate (**P**). The putative ferric–peroxy species appears earlier than the peroxy intermediate found by resonance Raman spectroscopy [reviewed in Babcock and Varotsis (1993)]. In the latter measurements, compound **A** disappeared with a rate consistent with the second kinetic phase observed here, but the Raman-visible ferric–peroxy compound only appeared later (160–220 μs). In order to explain this, it was proposed that the ferrous–oxy compound (**A**) is converted to a ferric–peroxy intermediate, but one that is invisible to resonance Raman spectroscopy until it takes up a proton later in the reaction. Hence, the 430-nm peak observed here can be assigned to this Raman-invisible ferric–peroxy compound—the first clear observation of this intermediate in the reaction of the fully reduced enzyme with oxygen.

A Model of the Initial Steps of Oxygen Activation. In order to explain these and other recent findings, we have developed a new model for the early steps in the oxygen reaction. The proposed sequence of intermediates is shown in Figure 4 (other parts of the figure illustrate a thermodynamic picture that will be developed below). The essential point in the model is that the initial steps of oxygen binding and reduction take place at equilibrium, and it is only with the arrival of an electron from Fe_a (the third electron in the oxygen reaction) that an energetic step commits the reaction to its forward course.

One important motivation for proposing a model of this kind is that it now seems that the rate of oxidation of Fe_a in the flow–flash reaction (the second phase in the present experiments) depends not only on the oxygen concentration (Hill & Greenwood, 1984) but *also* on factors that affect the inherent rate of electron transfer between the two hemes. This finding was made possible by the fact that cytochrome *o*, a bacterial enzyme that is closely homologous to cytochrome aa_3, can incorporate different types of hemes in its low-spin heme site (Puustinen et al., 1992). Two forms of the enzyme have been found: one with heme B at the low-spin site (cytochrome bo_3) and one with heme O (cytochrome oo_3). In both cases, the oxygen-binding heme is heme O. We have recently shown that the nature of the heme at the low-spin site affects the inter-heme electron-transfer rate (Morgan et al., 1993). With heme B, the time constant is approximately 3 μs (cf. cytochrome *c* oxidase), but with heme O in the site, the rate is approximately 10 times slower.

This change in the electron-transfer rate also appears to have an effect on the kinetics of the oxygen reaction. In a flow–flash study with cytochrome *o* from a strain of *Escherichia coli* that is known to produce roughly equal amounts of cytochrome bo_3 and oo_3 type enzymes, Svensson and Nilsson (1993) reported two processes that had different rates but parallel oxygen dependencies. The faster process had a rate similar to that of the present 32-μs phase and a maximum absorbance difference at 562 nm (the spectral maximum for low-spin heme B). The other process was about 10 times slower and had a spectral maximum near 555 nm, which is close to the spectral maximum for low-spin heme O. We suggest, therefore, that the two flow–flash phases observed by Svensson and Nilsson (1993) may be due to subpopulations of enzyme containing heme B and heme O, respectively, in the low-spin site. This leads directly to the conclusion that the rate of the 32-μs phase in the flow–flash reaction depends not only on the oxygen concentration but also on the inherent electron-transfer rate between the enzyme's two hemes, even though the time constant of the latter is only about 3 μs (Oliveberg & Malmström, 1991; Verkhovsky et al., 1992), and essentially requires a reaction scheme in which the reaction of oxygen with the enzyme is reversible, up to the point where the electron from Fe_a is transferred to the oxygen-binding site.

In the model (Figure 4), the fast (8 μs) phase of the reaction consists of the binding of oxygen to form an equilibrium mixture of the intermediates **R**, **B**, and **A**, together with a relatively unstable peroxy or superoxy intermediate (**P/S**), which is thus present at low occupancy. The enzyme remains in this equilibrium, which is dominated by the most stable intermediate, **A**, until the second (32 μs) phase, when an electron arrives from Fe_a, trapping the system as the lower energy intermediate, **P1** (presumably the unprotonated ferric–peroxy species described above). The low occupancy of the **P/S** intermediate explains the fact that oxidation of Fe_a and

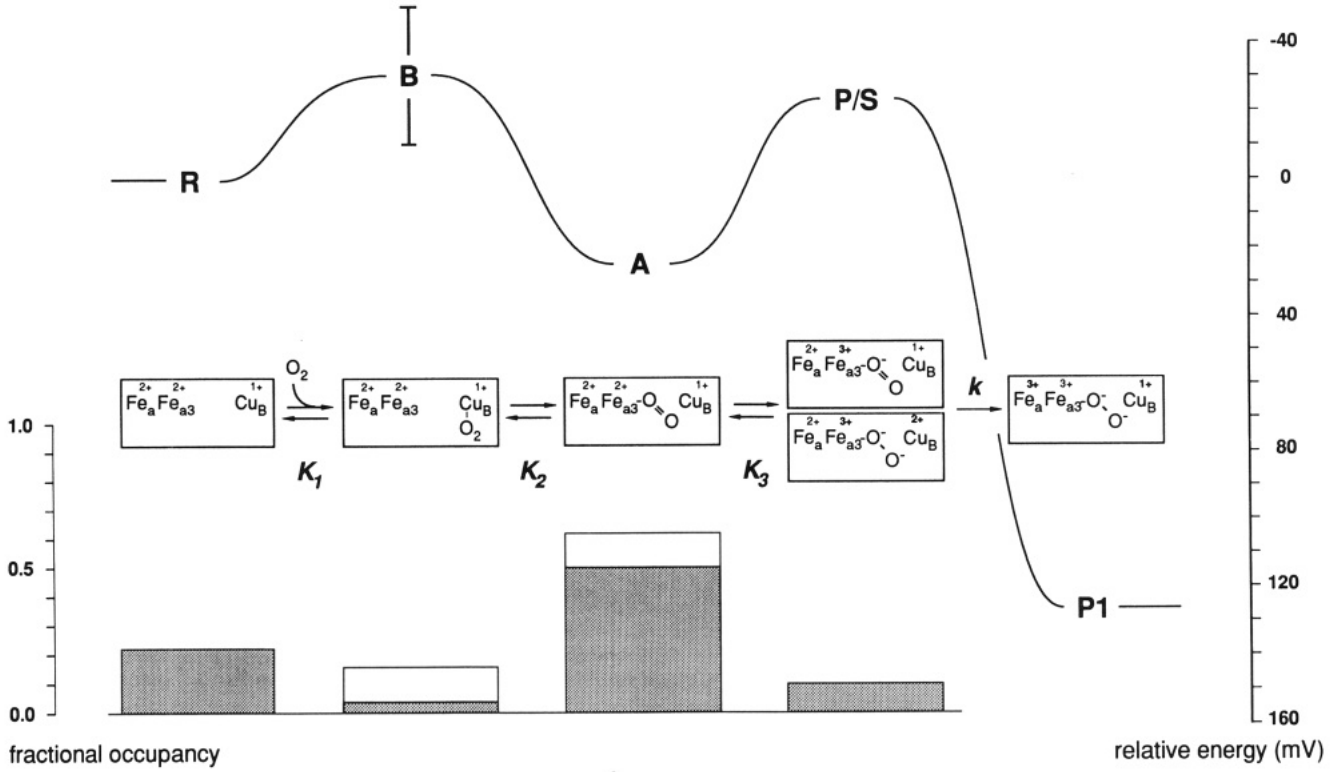

FIGURE 4: Model for the first steps in the reaction of fully reduced cytochrome *c* oxidase with oxygen. The series of boxes across the middle of the figure shows the structures of the proposed intermediates. Above or below each box is a letter that designates the intermediate (**R**, **B**, **A**, **P/S**, or **P1**).[2] The vertical position of each letter represents the relative energy level (millivolt scale) of the corresponding intermediate, as estimated in the model (see text). The bar graph below the first four intermediates shows their fractional occupancy at equilibrium. K_1, K_2, and K_3 are equilibrium constants, while k is the rate constant for inter-heme electron transfer. The bar at **B** indicates the upper and lower limits for the energy levels (see text). The corresponding bar for **A** would be smaller than the height of the symbol. The upper and lower limits in the equilibrium populations of **B** and **A** are indicated by the open and shaded rectangles in the bar chart. (Note that the larger occupancy at **B** would correspond to the smaller occupancy at **A**, and vice versa.)

formation of the ferric–peroxy species take place with a time constant of 32 μs, in spite of the fact that the time constant for electron transfer between the two hemes, measured directly, is 10 times as fast (Oliveberg & Malmström, 1991; Verkhovsky et al., 1992).

Although we do not observe intermediate **B**, there is some evidence for its existence. It was first proposed by Woodruff and co-workers (1991), when they observed that CO first binds to Cu_B and only then jumps to Fe_{a3}. More recently, Oliveberg and Malmström (1992) have reported absorbance changes at 830 nm, with the same rate as our fastest phase, which appear to reflect this binding of oxygen to Cu_B.

P/S is a purely hypothetical intermediate. We have given two possible formulas for this intermediate: a peroxy and a superoxy structure. In the former case, oxygen would accept two electrons from Fe_{a3} and Cu_B. In the latter case, a subpopulation of the ferrous–oxy intermediate would form a superoxide-like species by shifting electron density from the heme iron to oxygen. [In a theoretical study, Loew (1983) postulates such a substate for oxyhemoglobin, describing it as a low-lying triplet state.] In this version of the mechanism, Cu_B would never become oxidized during this part of the reaction. In either case, this **P/S** intermediate represents the first point in the scheme where Fe_{a3} is in its oxidized form, enabling electron transfer from Fe_a to take place.

Consistent with the model, we observe two clear kinetic phases, the first of which has a spectrum consistent with the formation of an equilibrium of states that is dominated by the ferrous–oxy intermediate (**A**). The amplitude of the fast phase itself suggests the formation of an equilibrium system. As described above, comparison of the spectrum of this phase to the spectrum of CO photolysis (Figure 3A) shows that not all of the unliganded enzyme created by the laser flash is converted into other species during this first phase of the reaction. It thus appears that in this equilibrium a significant amount of the enzyme remains in the form of **R**. The second phase has a spectrum consistent with the trapping of the enzyme population as a ferric–peroxy intermediate simultaneously with the oxidation of Fe_a. The trough at 445 nm can be assigned to the disappearance of at least a portion of Fe_a(II) and of the remaining **R** from the equilibrium system. As described above, the peak at 430 nm can be assigned to the formation of **P1**. The appearance of Fe_a(III) at 425 nm is apparently offset by the simultaneous disappearance of compound **A** in this phase.

The model also predicts that, since they are part of the same equilibrium system, intermediates **B** and **P/S** should be formed and should disappear with the same rates as compound **A**. Our instruments would not be able to observe either of these species, but it is interesting to note that the near-infrared absorbance, which Oliveberg and Malmström (1992) assign to intermediate **B**, appears and then disappears in parallel with our observation of compound **A**.

Thermodynamic Analysis. At this point, enough data are available to make estimates of the equilibrium constants in the model. This analysis does not give exact results, but nevertheless leads to a useful self-consistent picture of the early part of the oxygen mechanism. One important assumption about electron-transfer rates is required, as will be explained here.

Figure 5 shows the oxygen concentration dependence of various rate constants in the flow–flash reaction. The upper

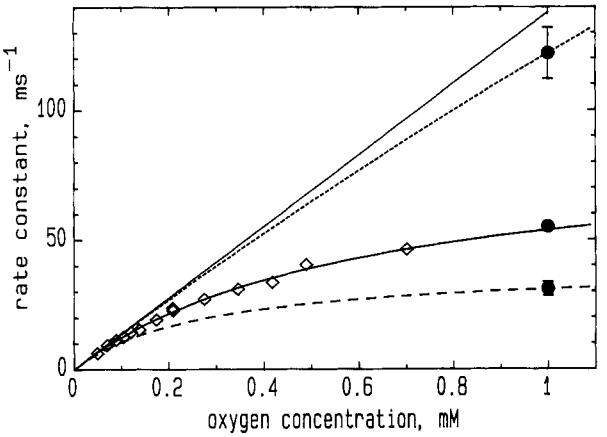

FIGURE 5: Oxygen concentration dependence of rates in the flow–flash reaction. The upper and lower black circles indicate the fast and slow phases, respectively, from our data. The middle black circle represents the apparent rate obtained from forcing a single-exponential fit onto our data for 445 nm. The ◇'s are the rates from the published data of Orii (1984, 1988b) for a similar single-exponential fit to 445-nm flow–flash data. The solid curve is the result of a hyperbolic function fit to the ◇ ($K_{D,app}$ = 1.6 mM). The upper solid line is an extrapolation of the initial slope of this binding curve, which reflects the bimolecular rate constant for the interaction of oxygen with the enzyme ($k = 1.38 \times 10^8$ M^{-1} s^{-1}). The two dashed curves are hyperbolic functions that pass through the points for the fast and slow phases, assuming the same bimolecular rate constant (K_1 = 8 mM and $K_{D,app}$ = 0.28 mM). Error bars indicate a ±2 standard deviation uncertainty in the fit.

and lower solid circles represent the fast (1.22×10^5 s^{-1}) and slow (0.31×10^5 s^{-1}) phases, respectively, from our data. As shown in Figure 1, these rates were obtained from kinetic traces at different wavelengths, where the two phases can be observed without mutual interference. In order to understand these rates, however, it is necessary to know the bimolecular rate with which oxygen originally interacts with the enzyme, and for this we need information about the kinetics of the reaction at very low oxygen concentrations. Some very good oxygen dependence data have been published, but unfortunately, the published rates are for experiments in which the two phases were not resolved. This is because the measurements generally have been made at 445 nm (the maximum wavelength for the reduced hemes), a wavelength where both phases contribute strongly, and because even at high oxygen concentration the two phases are not well-separated in time (see Figure 1B). However, at very low concentrations of oxygen, the bimolecular reaction is the rate-limiting step for the entire system, and thus a rate constant determined from single-exponential data should, nevertheless, give the correct value.[3]

A set of single-exponential rate constants of this kind is shown by the diamonds in Figure 5 (Orii, 1984, 1988b). The solid curve passing through these points shows the result of our fitting a simple binding (hyperbolic) function to these data. In order to check the compatibility of these results with ours, we made a similar single-exponential fit to our 445-nm data. The result is given by the third black circle (middle). This point falls on the curve derived from the earlier data, confirming the consistency of these results. The slope of this curve at zero oxygen concentration gives the bimolecular rate for oxygen reacting with the enzyme, denoted by the solid straight line. At very low concentrations of oxygen, this bimolecular reaction is the rate-limiting step for the entire system, and thus the oxygen dependence curve for any subsequent process must ultimately return to this asymptote. Given this bimolecular rate constant, we were able to estimate oxygen dependence curves for our first and second phases, shown by the short- and long-dashed curves, respectively.

Our rate for the second phase is much smaller than the bimolecular constant (the lower black dot lies well below the straight line), indicating a strongly hyperbolic dependence on oxygen concentration and indicating that oxygen is bound reasonably tightly to the enzyme prior to this phase of the reaction. The apparent dissociation constant ($K_{D,app}$) is 0.28 mM, which is in good agreement with the value reported by Hill and Greenwood (1984).

In the case of the fast phase, there also appears to be a hyperbolic dependence on oxygen concentration (the upper black dot is also below the straight line), and a similar analysis yields an apparent dissociation constant (K_1) of 8 mM. This suggests that oxygen does, in fact, bind to Cu_B en route to Fe_{a3} (intermediate **B** in the model), although the value for K_1 can only be taken as an upper limit, and binding may be tighter.[4] We will first calculate the equilibrium constants in the model using this upper limit value and then return to this calculation using an approach that will yield a lower limiting value.

According to the model (Figure 4), the apparent rate constant for the second phase (k_{app}) will depend on the oxygen concentration:

$$k_{app} = k/(K_1K_2K_3/[O_2] + K_2K_3 + K_3 + 1) \qquad (1)$$

K_1 is the apparent dissociation constant for the first phase, for which we have the value of 8 mM as an upper limit, and k is the rate constant for the step from intermediate **P/S** to **P1**. The value of k can be estimated from the results of direct electron-transfer measurements: When **P/S** is converted to **P1**, the electron moves from Fe_a to either Cu_B or oxygen, but this process would be expected to include a step in which the electron tunnels from Fe_a to Fe_{a3}. Given that the heme-to-heme distance is significantly larger than the heme-to-copper distance (Stevens et al., 1979; Hosler et al., 1993), this inter-heme electron-transfer step might be expected to be rate-

[3] This is an "apparent" bimolecular rate constant, since it is not the initial mechanistic "on" rate for oxygen interacting with the enzyme (which would be k_1, the forward rate from **R** to **B**). According to the model (Figure 4), the slope of this line will be $k/(K_1K_2K_3)$, since the process measured at 445 nm can be thought of as a prior equilibrium followed by kinetic rate limitation at the **P/S** to **P1** transition. Since this step essentially goes to completion, measured rate constants for the second phase have the character of "actual" and not "apparent" rate constants, in the sense that they reflect true "flow" from intermediate to intermediate in the system and are not just relaxation time constants. (A relaxation rate constant can potentially take on values larger than the flow.) As the oxygen concentration approaches zero, this flow is ultimately rate-limiting for all steps in the reaction. Thus, the apparent bimolecular constant derived from these data can be used to analyze other measured rates for steps in the overall reaction, provided that they also reflect flow in the system and are not apparent rate constants. For simplicity, we will continue to refer to this as the bimolecular rate constant.

[4] As with the second phase, we can define an apparent bimolecular constant for the first phase, equal to the slope of the straight line in Figure 5, by assuming that intermediates **R** and **B** are in fast equilibrium. This apparent bimolecular constant for the fast phase is k_2/K_1, where k_2 is the mechanistic forward rate constant from intermediate **B** to intermediate **A**, the parameter which controls forward flow at this point in the system. However, unlike the second phase, the measured (apparent) relaxation rate constant for the fast phase can potentially take on values that are larger than k_2/K_1. This is because the fast phase process does not go to completion, and thus the apparent rate constant may include contributions from other rate constants in the system, most importantly k_{-2}, the reverse rate constant (i.e., from intermediate **A** to intermediate **B**). Thus, the measured rate for the fast phase represents an upper limit on the value needed to determine binding at intermediate **B**, and the dissociation constant determined from the fast phase rate gives an upper limit for the true value (binding of oxygen to Cu_B is at least this tight).

limiting overall. This is supported by the results from cytochrome *o*, discussed above, which show that factors that affect the rate of heme–heme electron transfer also affect the rate of this phase of the flow–flash reaction. On this basis, we have used a previously determined rate constant for the inter-heme electron transfer, 0.24×10^6 s^{-1} (Verkhovsky et al., 1992), as an approximate value of k.

This value for the inter-heme electron-transfer rate was measured under circumstances where Fe_{a3} is 5-coordinate, high-spin (Oliveberg & Malmström, 1991; Verkhovsky et al., 1992), whereas when **P/S** is converted to **P1** in the oxygen reaction, Fe_{a3} would be 6-coordinate, low-spin, with the oxygen intermediate as the sixth ligand. As such, the driving force and rearrangement energy for the electron transfer could be different. It is important to note, however, that the driving force for the heme-to-heme electron tunneling event per se is *not* equal to the energy difference between **P/S** and **P1**. The fact that the electron transfer ultimately leads to highly energetic oxygen chemistry would not, in itself, be expected to alter either the driving force or the rearrangement energy for the electron transfer, since the oxygen chemistry takes place only after the electron has moved (Gelles et al., 1986).

The model also leads to the following equation for the apparent dissociation constant for the second phase ($K_{D,app}$), the value of which is estimated above:

$$K_{D,app} = K_1K_2K_3/(K_2K_3 + K_3 + 1) \quad (2)$$

Using the above values for $K_{D,app}$, K_1, and k, we can solve the two equations simultaneously to arrive at values of $K_2 = 0.044$ and $K_3 = 4.8$, on the basis of the upper limiting value of K_1. This leads to the following populations of intermediates after the fast phase: [**R**] = 22%, [**B**] = 3%, [**A**] = 62%, and [**P/S**] = 13%.

We can also approach this analysis in terms of a lower limiting value for K_1 by using the spectrum of the fast phase reaction (Figure 3). The quantity ([**R**] + [**B**]) can be found from the difference between the amount of unliganded enzyme that appears after the photolysis (445 nm) and the amount that is seen to disappear in the fast phase. (In these spectra, **B** would be expected to look like **R**.) This gives a value of 37% for ([**R**] + [**B**]). As described above, this value is an upper limit on the amount of these two intermediates.

From the model, the following two relationships can be derived:

$$[\mathbf{R}] = K_{D,app}/(K_{D,app} + 1) \quad (3)$$

$$[\mathbf{P/S}] = k_{app}/k \quad (4)$$

Given the values of $K_{D,app}$ and k_{app} above, this leads to values of [**R**] = 22%, [**P/S**] = 13%, and [**B**] = 15%. Since at this point in the reaction,

$$[\mathbf{R}] + [\mathbf{B}] + [\mathbf{A}] + [\mathbf{P/S}] = 100\% \quad (5)$$

we can arrive at values for the populations of all four intermediates, [**R**] = 22%, [**B**] = 15%, [**A**] = 50%, and [**P/S**] = 13%, and thus find the equilibrium constants, $K_1 = 1.5$ mM, $K_2 = 0.3$, and $K_3 = 3.8$. Note that, in this new analysis, the values of [**B**] and [**A**] have changed, while [**R**] and [**P/S**] remain the same.

These values for K_1, K_2, and K_3 allow us to estimate the relative energy of the states in the equilibrium system created by phase 1. As shown in Figure 4, the energetic relationships are indicated by the levels of the intermediates in the reaction curve. The relative populations of the equilibrium species (i.e., not including **P1**) are shown by the bar chart in the lower left of the figure. In both cases, the upper and lower limits for **B** and **A**, from the above calculations, are indicated. The location of **P1** relative to the other states represents an estimate of the difference between the redox midpoint potentials of Fe_a and Cu_B and, thus, reflects an assumption that the actual intermediate is peroxy-like and not superoxy-like. As discussed above, this estimated energy difference between **P/S** and **P1** is not the relevant energy for evaluation of the inter-heme electron tunneling process that takes place as part of this overall step.

In order to carry out this analysis, we have made assumptions about the inter-heme electron-transfer rate and the equilibration of binding steps prior to the observed kinetic phases. Nevertheless, this should not affect the overall picture of the reaction that comes from this analysis: (1) the first phase of interaction of oxygen with the enzyme produces a quasi-equilibrium of states; (2) there is almost certainly initial binding of oxygen to Cu_B (intermediate **B**); (3) oxygen binding to Fe_{a3} (intermediate **A**) is much tighter, with the result that this intermediate dominates the difference spectrum of the fast phase; and (4) a significant fraction of the enzyme remains in the unbound state (**R**) in this equilibrium. Perhaps the most significant point is the low occupancy of the putative peroxy or superoxy intermediate (**P/S**), which accounts for the fact that the oxidation of Fe_a in the flow–flash reaction is so much slower than the measured inter-heme electron-transfer rate.

Interestingly, the model also accounts for some flow–flash results which, up to this point, have been somewhat problematic. In the reaction of the fully reduced enzyme, the intermediate that is observed, before the third electron arrives in the oxygen-binding site, is a ferrous–oxy compound (Varotsis et al., 1989; Orii, 1988a), in spite of the fact that enough reducing equivalents are present in the catalytic site to form a ferric–peroxy compound, an intermediate which is only observed *after* the third electron arrives (Varotsis et al., 1989). This finds a natural explanation in the present model: The reaction actually *does* produce a partially reduced oxygen intermediate (**P/S**) before the third electron arrives, but it coexists with the ferrous–oxy intermediate (**A**), which has a much higher occupancy and thus dominates the spectrum.

A similar phenomenon is observed when the starting material is the two-electron-reduced, CO-mixed-valence enzyme. The fastest phase of this reaction appears to be the same as in the case of the fully reduced enzyme: The rate constant is about 90×10^3 s^{-1} (Oliveberg et al., 1989), and the intermediate that is observed after this phase has been identified by both resonance Raman (Babcock & Varotsis, 1993) and visible spectroscopy (Hill & Greenwood, 1983) as a ferrous–oxy compound (**A**). However, in this case there is no phase that would correspond to the second phase in the reaction of the fully reduced enzyme, and the next observed kinetic phase has a rate constant of about 6×10^3 s^{-1} (Hill & Greenwood, 1983; Oliveberg et al., 1989). Thus, without the third electron, the ferrous–oxy intermediate (**A**) persists, even though the mixed-valence enzyme contains enough electrons to produce a peroxy compound. The model predicts that, with only two electrons available for the reaction, the equilibrium, dominated by intermediate **A**, will be long-lived because there is no electron to trap the system in intermediate **P1**. A stable peroxy compound will be produced quickly, only if a third electron is available in the low-spin heme.

Outlook. This study has confirmed the formation of a ferrous–oxy compound (**A**) as a product of the first reaction

phase and has provided the first clear evidence of a ferric–peroxy intermediate as the direct product of the second reaction phase. The data support the suggestion that oxygen binds weakly to Cu_B en route to Fe_{a3} (Woodruff et al., 1991).

The actual nature of the intermediate designated **P1** in our scheme remains an interesting question. As described above, this is not the same intermediate that is observed in resonance Raman experiments in the 160–220-μs window. Babcock and Varotsis (1993) assign the Raman-visible peroxy intermediate as a protonated species and propose an unprotonated, Raman-invisible peroxy intermediate for the time at which we observe the 430-nm species. This still leaves open the question of how these two putative intermediates relate to the peroxy intermediate observed in experiments in which the oxygen reaction is driven backward in energized mitochondria (Wikström & Morgan, 1992).

Intermediate **P/S** remains the unique prediction of our model, and observation of such an intermediate at the appropriate time would constitute strong corroboration. Unfortunately, detection of this species can be expected to be difficult, given the low relative occupancy and short lifetime predicted.

ACKNOWLEDGMENT

We thank Hilkka Vuorenma for skillful technical assistance, Martti Heikkinen for mechanical shop work, and Nickolai Belevich for help in design and construction of instruments.

REFERENCES

Babcock, G. T., & Wikström, M. (1992) *Nature 356*, 301–309.
Babcock, G. T., & Varotsis, C. (1993) *J. Bioenerg. Biomembr. 25*, 71–80.
Baker, G. M., Noguchi, M., & Palmer, G. (1987) *J. Biol. Chem. 262*, 595–604.
Chance, B., Saronio, C., & Leigh, J. S. (1975) *J. Biol. Chem. 250*, 9226–9237.
Gelles, J., Blair, D. F., & Chan, S. I. (1986) *Biochim. Biophys. Acta 853*, 205–236.
Gibson, Q. H., & Greenwood, C. (1963) *Biochem. J. 86*, 541–555.
Hartzell, C. R., & Beinert, H. (1974) *Biochim. Biophys. Acta 368*, 318–338.
Hill, B. C. (1991) *J. Biol. Chem. 266*, 2219–2226.
Hill, B. C., & Greenwood, C. (1983) *Biochem. J. 215*, 659–667.
Hill, B. C., & Greenwood, C. (1984) *Biochem. J. 218*, 913–921.
Hosler, J. P., Ferguson-Miller, S., Calhoun, M. W., Thomas, J. W., Hill, J., Lemieux, L., Ma, J., Georgiou, C., Fetter, J., Shipleigh, J., Tecklenburg, M. M. J., Babcock, G. T., & Gennis, R. B. (1993) *J. Bioenerg. Biomembr. 25*, 121–135.
Loew, G. H. (1983) in *Iron Porphyrins, Part I* (Lever, A. B. P., & Gray, H. B., Eds.) pp 3–88, Addison-Welsley, Reading, MA.
Morgan, J. E., Verkhovsky, M. I., Puustinen, A., & Wikström, M. (1993) *Biochemistry 32*, 11413–11418.
Oliveberg, M., & Malmström, B. G. (1991) *Biochemistry 30*, 7053–7057.
Oliveberg, M., & Malmström, B. G. (1992) *Biochemistry 31*, 3560–3563.
Oliveberg, M., Brzezinski, P., & Malmström, B. G. (1989) *Biochim. Biophys. Acta 977*, 322–328.
Orii, Y. (1984) *J. Biol. Chem. 259*, 7187–7190.
Orii, Y. (1988a) *Ann. N.Y. Acad. Sci. 550*, 105–117.
Orii, Y. (1988b) *Chem. Scr. 28A*, 63–69.
Puustinen, A., Morgan, J. E., Verkhovsky, M. I., Thomas, J. W., Gennis, R. B., & Wikström, M. (1992) *Biochemistry 31*, 10363–10368.
Stevens, T. H., Brudvig, G. W., Bocian, D. F., & Chan, S. I. (1979) *Proc. Natl. Acad. Sci. U.S.A. 76*, 3320–3324.
Svensson, M., & Nilsson, T. (1993) *Biochemistry 32*, 5442–5447.
Varotsis, C., Woodruff, W. H., & Babcock, G. T. (1989) *J. Am. Chem. Soc. 111*, 6439–6440.
Varotsis, C., Woodruff, W. H., & Babcock, G. T. (1993) *Proc. Natl. Acad. Sci. U.S.A. 90*, 237–241.
Verkhovsky, M. I., Morgan, J. E., & Wikström, M. (1992) *Biochemistry 31*, 11860–11863.
Vygodina, T. V., & Konstantinov, A. A. (1988) *Ann. N.Y. Acad. Sci. 550*, 124–138.
Wikström, M., & Morgan, J. E. (1992) *J. Biol. Chem. 267*, 10266–10273.
Wikström, M., Krab, K., & Saraste, M. (1981) *Cytochrome Oxidase: A Synthesis*, Academic Press, London.
Woodruff, W. H., Einarsdottir, O., Dyer, R. B., Bagley, K. A., Palmer, G., Atherton, S. J., Goldbeck, R. A., Dawes, T. D., & Kliger, D. S. (1991) *Proc. Natl. Acad. Sci. U.S.A. 88*, 2588–2592.